ECONTECHMOD. AN INTERNATIONAL QUARTERLY JOURNAL – 2016. Vol. 5. No. 2. 51–62

Using the finite element method in the modeling of layered composite delamination

K. Tucki

Department of Production Management and Engineering, Warsaw University of Life;
e-mail: karol_tucki@sggw.pl

Received April 17.2016: accepted June 21.2016

Abstract. The article presents issues associated with an analysis of the process of delamination of fibrous composite using the Finite Element Method. Research encompassed three computer modelling sessions for delamination of the material for three different values of distance between the test force application point and the middle of the laminate. The results, encompassing the force value and displacement, were then compared to identify the correlation between these variables and the distance from the force application point. The model correctness was also verified by comparing the value of forces modelled with the real values, obtained during an experiment.

On the basis of the results obtained with regard to the size of the force applied, it was concluded that the numerical model represented well the mathematical model presented by Comanho. The negative result errors were due to the increased sensitivity of the software to the laminate fracture phenomenon, occurring during the experiment. Thanks to good representation of the model, it can be used interchangeably with numerical calculations

Key words: composite, analysis, finite element method.

INTRODUCTION

The purpose of modelling is to develop mathematical models to describe the examined physical phenomena [2, 17, 19, 23]. The Finite Element Method (FEM) has become very popular in this regard [3, 4, 21, 22]. This article describes application of the Finite Element Method for modelling of layered composite (the phenomenon of delamination) [5, 10, 14, 27, 29]. Its objective is to analyze delamination along with the crack initiating such delamination [11, 13, 15, 31].

Modelling of delamination of layered composite was performed using the parameters and results of laboratory tests described in the article [7].

The actual laminate, used in the experiment, is a two-layered composite, placed on the base supporting both ends of the laminate. On the top there is a beam attached to the composite in two locations: in the middle and near the end, in which delamination is taking place. The beam is subject to the force of leverage of the value of F_{lp}. This value shifts the entire load applied to the composite, resulting in delamination of the material or lack of such delamination. The objective of this modelling is to obtain the maximum value of force F_{lp}. The actual model geometry is presented in Fig. 1.

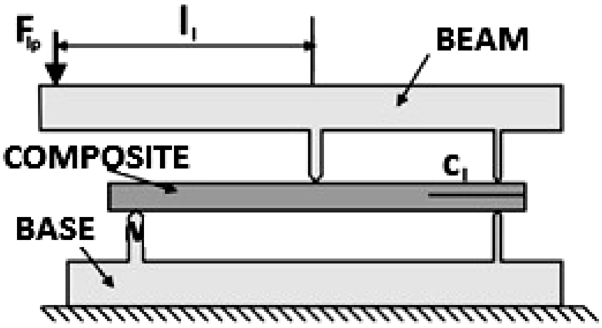

Fig. 1. The actual laminate geometry [Own elaboration on the basis of 7]

Leverage force was applied at the distance of l_l from the middle of the laminate. This distance influences the impact of individual fixtures of the beam on the composite. Depending on application of force F_{lp} to the beam, the ratio of the action of the force of the fixture in the middle of the laminate (the force acting down) and the forces at the end (the force acting up) of the laminate changes.

Simultaneous action of the two forces results in two types of loads: bending and stretching, which results in emergence of normal and shear stresses [1, 8, 24, 26, 32]. Normal stress emerges as the force acts at the end of the beam and it leads to delamination of the material. Shear stress results from impact in the middle of the beam.

Displacement due to development of a crack along the normal direction is referred to as mode I, and in the shear direction – mode II. Tests were conducted for the mixed mode, taking into account mode I and mode II. The emergence of the two modes depends on the above-mentioned action of leverage force. Correlation between the two modes in relation to displacement δ is presented in Fig. 2.

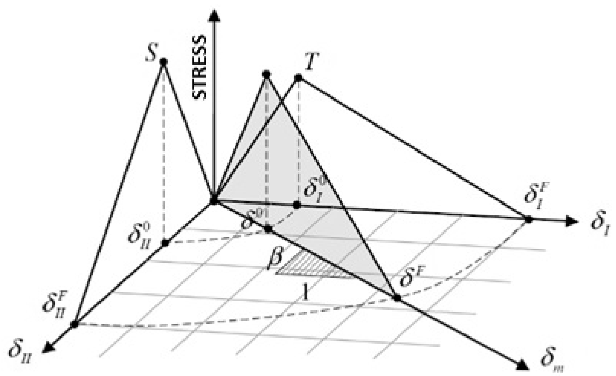

Fig. 2. Stress-displacement chart for the mixed mode, taking into account mode I and mode II [20]

The mixed mode coefficient β, visible in Fig. 2, defines the share of individual modes in the process. By changing the values of this coefficient, as well as the values of variables depending on β, three different modelling processes were obtained:

1. Modelling 1 for β=0,2;
2. Modelling 2 for β=0,5;
3. Modelling 3 for β=0,8.

All displacements with index ***I*** are applicable to mode I: δ_I, δ_{I0}, δ_{If}, while displacements with index ***II*** – to mode II: δ_{II}, δ_{II0}, δ_{IIf}. The remaining displacements are assigned to the mixed mode. For the purposes of this study, in order to facilitate recording of the calculations, instead of symbol δ, symbol ***u*** was applied.

Tests were conducted using simplified models, disregarding the leverage force. The models consist of two layers of laminate, where the length of one layer is 102 mm, its width is 25.4 mm and thickness – 1.56 mm, which, for two layers, gives the result of 3.12 mm. T geometry of the modelled laminate is presented in Fig. 3. In addition, Fig. 3 presents the length of the crack, which emerged in the middle of the laminate thickness. Supports were placed on both ends of the beam.

In the middle of the top side of the beam, there is the conventional leverage that shifts the load. The leverage is also fixed to the end, and it rotates around the area of contact towards the middle of the beam. The force id displaced towards the opposite free end, which allows for the application of mode I and II loads, simultaneously. In the model, the leverage was disregarded and replaced with direct forces. There are two forces acting on the model: tensile force F_e, applied at the end of the beam and compressive force F_m, applied in the middle of the beam.

The initial length of delamination of samples *cl* (Fig. 1) depending on coefficient β and resistance to cracking G_c,obtained in the experiment are presented in Table 1.

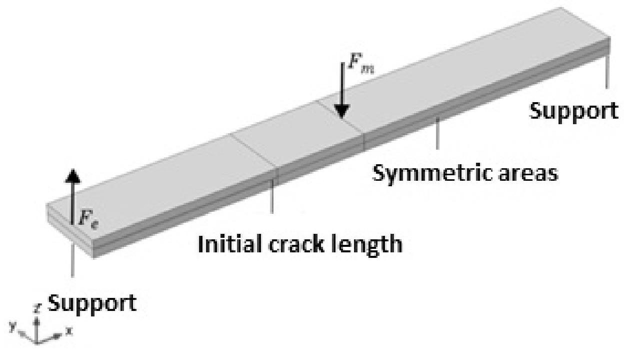

Fig. 3. Geometry of the laminate modelled [Own elaboration]

Table 1. Sample delamination length and resistance to cracking [7]

Mixed mode coefficient β	0,2	0,5	0,8
Resistance to crackingG$_c$ (kJ/m^2)	1,103	1,131	1,376
Delamination length cl (mm)	33,7	34,1	31,4

The material of which the laminate is made is fibrous carbon epoxy composite AS4/PEEK, where AS4 is the fiber, connected using epoxy resin PEEK [12]. The characteristics of this material are presented in Table 2.

Model development stages

13 main stages of the model development were distinguished, where the first 11 are responsible for the model development and the last two – for calculations and results [6, 16,28, 30, 33]. Modelling was conducted using the COMSOL software.

1. Introduction – specification of the modelling type.

Two types of physical phenomena were added, which served as the basis for laminate modelling: Solid Mechanics – for modelling of solids, andBoundary ODEs and DAEs – introduction of differential equations.

2. Parameters – specification of the main parameters of the model.

Table 2. Characteristics of composite AS4/PEEK [7]

Feature	Symbol	Value
Young's module	E_X	122,7 GPa
	E_Y=E_Z	10,1 GPa
Poisson's ratio	ν_{YZ}	0,45
	ν_{XY}, ν_{XZ}	0,25
Kirchoff's module	G_{YZ}	3,7 GPa
	G_{XY}=G_{XZ}	5,5 GPa
Density	g	1570 kg/m^3
Maximum tensile stress	N_s	80 MPa
Maximum shear stress	S_s	100 MPa
Connection rigidity	K_p	106 N/mm^3
Fracture energy - mode I	G_{Ic}	969 J/m^2
Fracture energy - mode II	G_{IIc}	1719 J/m^2

Parameters			
Name	**Expression**	**Value**	**Description**
lb	102[mm]	0.102 m	Length
wb	25.4[mm]	0.0254 m	Width
hb	2*1.56 [mm]	0.00312 m	Thickness
cl	34.1[mm]	0.0341 m	Initial fracture length
Kp	1e6[N/mm^3]	1.0000E15 N/m^3	Connection rigidity Maximum tensile stress
N_s	80[MPa]	8.0000E7 Pa	Maximum shear stress
S_s	100[MPa]	1.0000E8 Pa	Displacement initiating
u_I_0	N_s/Kp	8.0000E-8 m	Displacement initiating failure for mode I
u_II_0	S_s/Kp	1.0000E-7 m	Displacement initiating failure for mode I
GI_c	0.969[kJ/m^2]	969J/m^2	Failure energy for mode I
GII_c	1.719[kJ/m^2]	1719J/m^2	Failure energy for mode II
u_I_f	2*GIc/N_s	2.4225E-5 m	Displacement resulting in breaking of connection for mode I
u_II_f	2*GIIc/S_s	3.4380E-5 m	Displacement resulting in breaking of connection for mode II
eta	2.284	2.284	Benzeggagh and Kenane (BK) fracture criterion
disp	0	0	Displacement parametr
b	0.5	0.5	Mixed mode coefficient
II	lb/2*(0.5*sqrt(3*1-b)/b)+1)/(3-0.5*sqrt(3*(1-b)/b))	0.044596	Distance from load point
Ir	8*((6*b+sqrt(3*b*(1-b)))/(3+9*b+8*sqrt*3*b*(1-b))))	2.1436	Average load coefficient

Fig. 4. Basic model parameters for β = 0,5 inCOMSOL [Own elaboration]

Table 3. Dimensions of individual blocks [Own elaboration]

No.	Specification	Block I	Block II	Block III
1	Length	cl	lb/2-cl	lb/2
2	Width	wb/2	wb/2	wb/2
3	Thickness	hb	hb	hb
4	Layers	Layer 1- hb/2	Layer 1- hb/2	Layer 1- hb/2

Fig. 4 presents the basic parameters for the model being developed. Most of them are common for all the three models. Values that vary are marked by the red frame and they include: initial fracture length *cl*, mixed mode coefficient *β*, distance from loading point *ll* and medium load coefficient *lr*.3. Model geometry – development of the model on the basis of the parameters specified.

The geometric model was built of two identical layers, adjacent to one another along the largest plane (Table 3). However, in order to define the model property and facilitate identification of the required load points, the laminate was made of three double blocks. Moreover, the laminate was built of one half of its width *wb/2*, which allowed for the application of the forces exactly in the middle of the actual laminate, and in the case of the model – on one of the sides.

4. Definition of the Cohesive Zone Model – specification of the areas, on which CZM was used (the place of connection of the two layers), and its parameters; specification of variables for the load point originating from leverage;

5. Material – selection of the type of material and specification of its parameters;

6. Definition of the Thin Elastic Layer – specification of forces acting in the Thin Elastic Layer; introduction of the model symmetry.

The first stage of the specification of the model mechanics consists of defining the *Thin Elastic Layer*. For this purpose, the *Thin Elastic Layer* was selected from the *Physics* toolbar. This layer is used for cohesive areas, defined in the previous points. The parameter indicated was the *Force per area as function of extension* F_A. In the calculation software, loads acting on each axis were entered, calculated as the product of cohesive displacement present at a given axis and cohesive rigidity. If u_I<0,along axis Z, instead of cohesive rigidity, rigidity of the entire material K_p was applied.

7. Load definition – specification of forces acting on the model.

The next step was specification of the forces acting on the model (F_e and F_m), associated with leverage (Table 4).

8. Expected displacement – blocking of displacement in undesirable directions.

The operation, which enforces specific displacement or prevents displacement of the model in undesirable direction, is *Prescribed Displacement* in the *Physics* section. The last operation, performed in the section *Solid Mechanics*, is specification of the global equation for the general force used earlier to define the loads and the load point force (Fig. 5).

Table 4. Defining of loads F_e and F_m [Own elaboration]

	tensile F_e	shear F_m
x	0	0
y	0	0
z	force	-lr*force

9. Boundary ODEs and DAEs – entering of differential equations in the model; introduction of discretization in the cohesive areas; specification of displacement.

10. Model discretization – application of mesh to the model.

All operations associated with discretization of the model were performed in the *Mesh* section, automatically added to the *Model Builder* tree.

The system generated the following values:

– maximum component size 0,00204 m,
– minimum component size 0,0000204 m,
– maximum increase rate for component 1,3,
– curve coefficient 0,2,
– narrowness resolution 1.

The above values are applicable to distribution of components along the X axis. The maximum and minimum component size depends on the length of the laminate and it is subsequently 50 times smaller for the maximum size and 5000 times smaller for the minimum size.

The graphic model with all the discretization changes made is presented in Fig. 6.

11. Test type – introduction of the calculation algorithm.

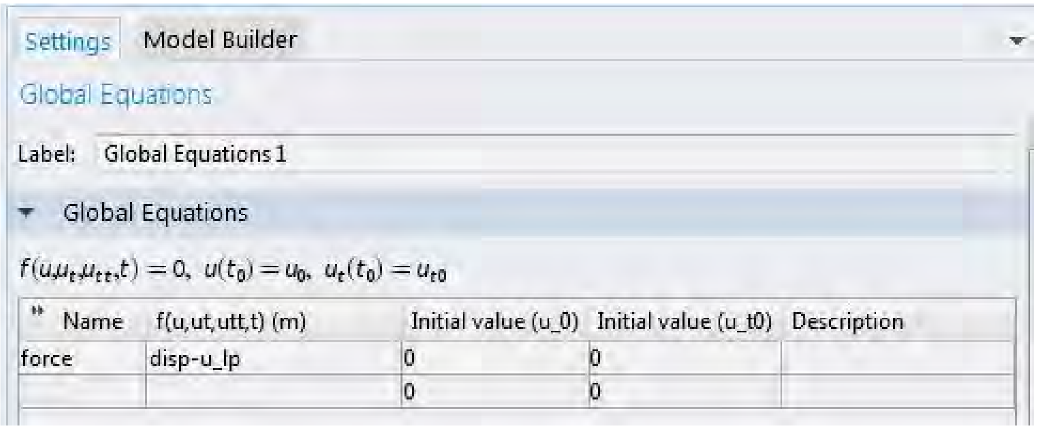

Fig. 5. Specification of *force* in COMSOL [Own elaboration]

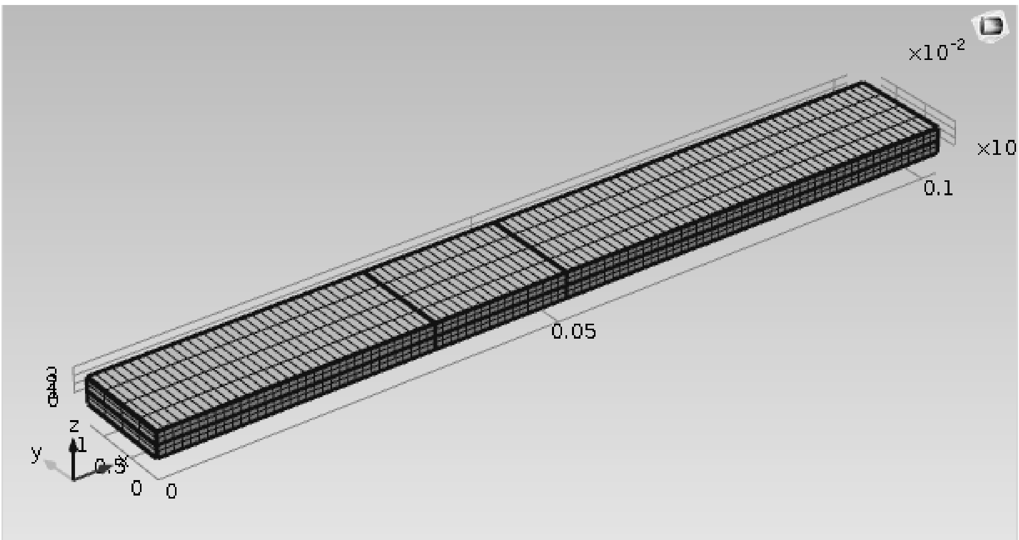

Fig. 6. The model mesh distribution in COMSOL [Own elaboration]

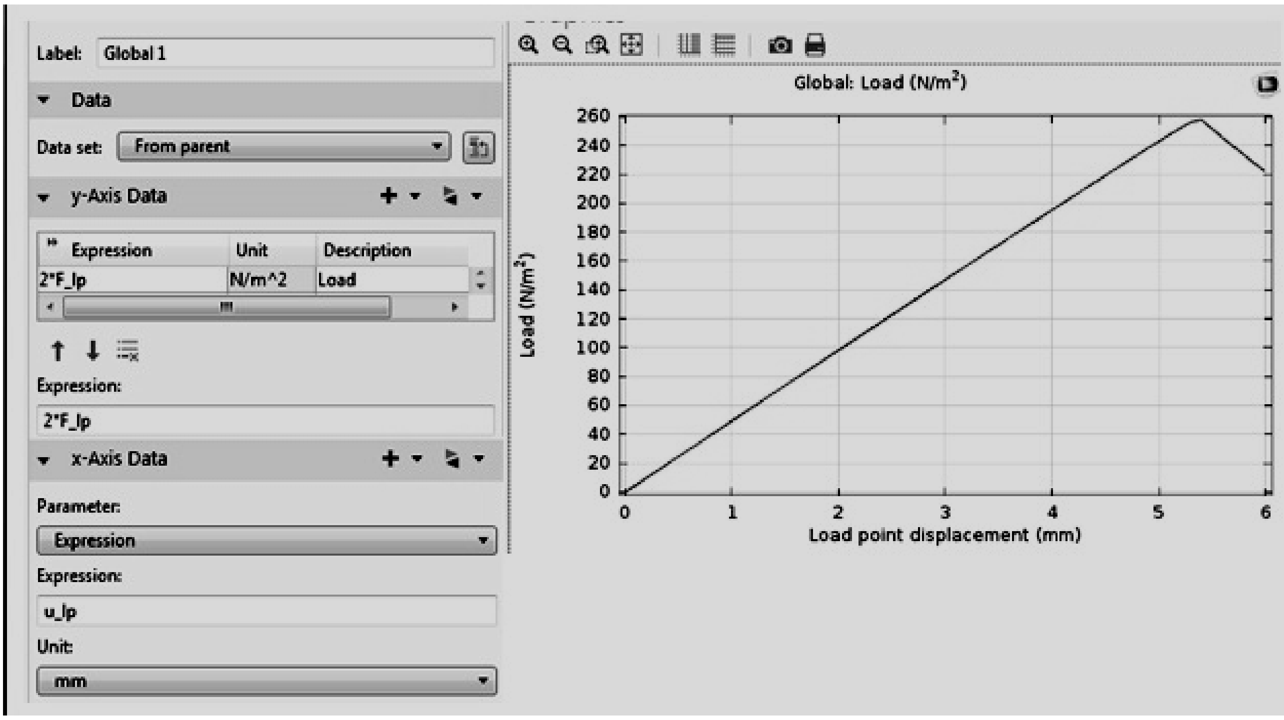

Fig. 7. The model mesh distribution in COMSOL [Own elaboration]

Table 5. Calculation times for three different experiments [Own elaboration]

	β = 0,2	β = 0,5	β = 0,8
Calculation time (min)	24 min 11 s	33 min 10 s	47 in 29 s

Table 6. Coefficients of varying value for individual experiments [Own elaboration]

Feature	Symbol	Exp. 1	Exp. 2	Exp. 3	Mode of obtaining of value
Mixed mode coefficient	β	0,2	0,5	0,8	By experiment
Distance from load point	l_l	0,1098	0,0446 m	0,0285 m	Formula based calculations
Average load coefficient	l_r	1,4641	2,1436	2,7913	Formula based calculations
Initial fracture length	c_l	0,0337	0,0341	0,0314 m	By experiment

This is the last stage before the commencement of computer calculations. The objective is to configure and enable the tracking of maximum displacement in the mixed mode. Test specification started by defining the *Stationary* used earlier – it is responsible for the selection of the model geometry type (linear or non-linear) and the size of displacement between layers. In the *Stationary* options, nonlinearity of geometry was included, which requires marking of the option *Include geometric nonlinearity*. Discretization changed the model analyzed from linear to discrete, hence the selection of the above option. *Auxiliary Sweep* was also selected, which is an auxiliary calculation algorithm, used, when there are no geometric changes in the model. The parameter, which is to be used in the calculation algorithm, is interlayer displacement (*disp*).

12. Computer-aided calculations.

Three different calculations were conducted for three different mixed mode coefficients β, for which duration times and the number of degrees of freedom solved are provided in Table 5.

13. Generating of charts.

The chart generated presented a simulation of delamination and deformation of laminate, and the second chart presented laminate deformation on a two-color scale. Moreover, a linear chart was generated, presenting the *Load – displacement curve* (Fig. 7).

The chart from Fig. 7 presents the load force value, which is the purpose of the calculations. It can be read from the chart or generated. From the *Results* toolbar, *Global Evaluation* was selected. The searched value of *2*F_lp* was entered and marked as *Maximum*. In this manner, the maximum value of the beam load force, which does not lead to fracture of the laminate, was identified.

Test results

The experiments conducted varied in terms of the value of the mixed mode coefficient β.

Table 6 presents coefficients with values, which were different for different models. In the right column of the table, information on how a given value was obtained can be found.The last stage in the model development was associated with generation of charts on the basis of results obtained during calculations. For each of the three experiments, varying in terms of the mixed mode coefficient β,3 different charts were obtained:

- the model stress chart;
- the model deformation chart;
- the displacement shift curve chart and the constant initiating laminate delamination;
- the load force value.

The displacement shift curve chart

The charts provided below (Fig. 8–10) illustrate the correlation between the load force F_{lp} and leverage displacement. In both cases, as the load force increases, the leverage moves down, and this displacement is growing proportionally. The force value is growing linearly until the delamination of the laminate. From this point on, the force value starts to decrease non-linearly. This is due to the fact that the further part of the process is past the most difficult stage, which is complete delamination of the laminate from the place of fracture in the direction of the point of application of force F_e.

The charts presented, as well as Table 7, indicate that the delamination took place the fastest in experiment 3, and the beam was shifted by 5 mm in relation to its original position. In this case, the force applied was displaced at the smallest distance from the middle l_l = 0,028 m. The delamination was the latest – after 10 mm, in experiment 1. In this case, the distance between the force applied and the middle of the model was 0,110 m.

A similar phenomenon can be observed in the case of the force applied. The highest values were observed for experiment 3 (473,17 N), and the lowest – for experiment 1 (58,64 N) (Table 8). The difference in values between the two experiments is as much as 8-fold.

Summing up, as the distance between the load point and the middle of the laminate increases, so does the displacement of the load, while the force to be applied to delaminate the composite material decreases.

Table 7. Load and load point displacement values for individual experiments [Own elaboration]

		Experiment 1	Experiment 2	Experiment 3
Maximum load	F_{lp}	58,64 N	257,87 N	473,17 N
Displacement for maximum load	u_{lp}	0,01 m	0,0054 m	0,005 m
Load point distance	l_l	0,10989 m	0,044596 m	0,028471 m

Table 8. Real and modelled load values [Own elaboration on the basis of 7]

	Experiment 1	Experiment 2	Experiment 3
Real	99,90 N	274,50 N	502,00 N
Modelled	97,73 N	257,87 N	473,17 N
Error	-2,17 %	-6,06 %	-5,74 %

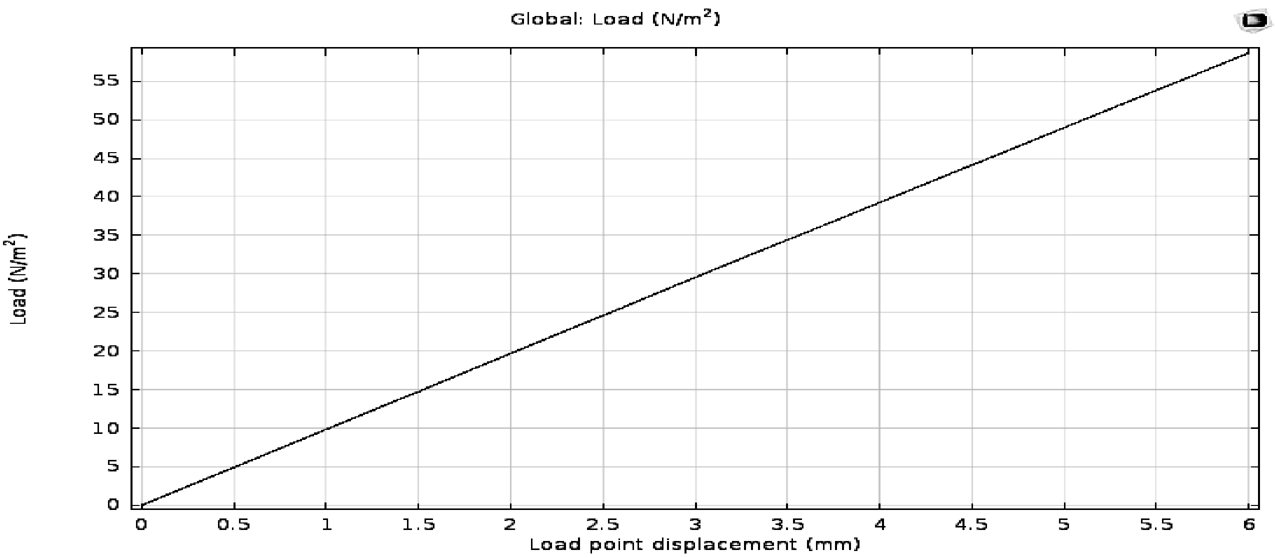

Fig. 8. The displacement shift curve chart for β=0,2 in COMSOL [Own elaboration]

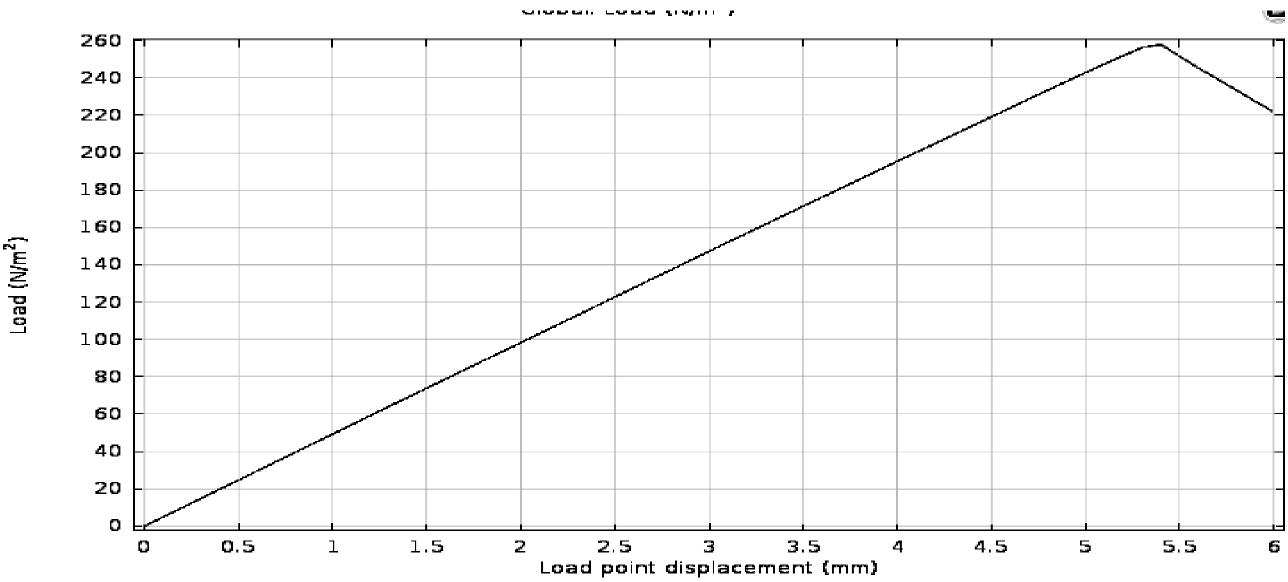

Fig. 9. The displacement shift curve chart for β=0,5 in COMSOL [Own elaboration]

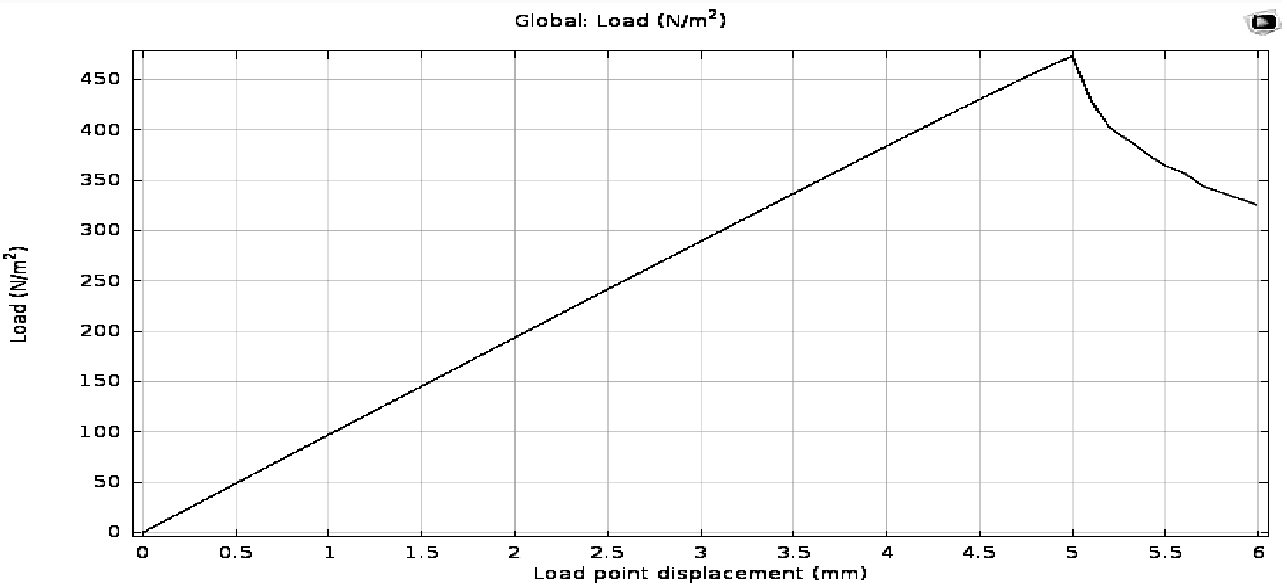

Fig. 10. The displacement shift curve chart for β=0,8 in COMSOL [Own elaboration]

Data for the model were obtained on the basis of a real experiment, which was conducted for the composite of the same dimensions, the same properties and with the same load system [7]. Values of the maximum load to be applied to the beam were obtained and presented in Table 8 along with the values modelled. 8.The results obtained in the modelling are similar to those obtained in the real experiment. However, in every case their value is somewhat lower. This is due to the fact that in computer modelling more attention was paid to the initiation of fracture prior to delamination, by introduction of the Cohesive Zone Model.

The model stress charts

The stress charts (Fig. 11–13) were developed on the basis of displacement u_{lp} for the maximum load value. In order to model a well-visible delamination, 10-fold displacement was applied. This resulted in a substantial increase in the distance between the top layer and the bottom layer.

The most visible bending of the beam was observed in experiment 3 (Fig. 13), and the smallest – in experiment 1 (Fig. 11). Differences in material bending are caused by different force values, described for the previous charts. The higher the force value, the greater the model stress value.

The model deformation chart

The size of the area subject to delamination is illustrated much better by the model deformation charts (Fig. 14–16).

Maximum delamination, which may take place, is the delamination of one half of the laminate. In the middle, the downforce prevents further delamination.

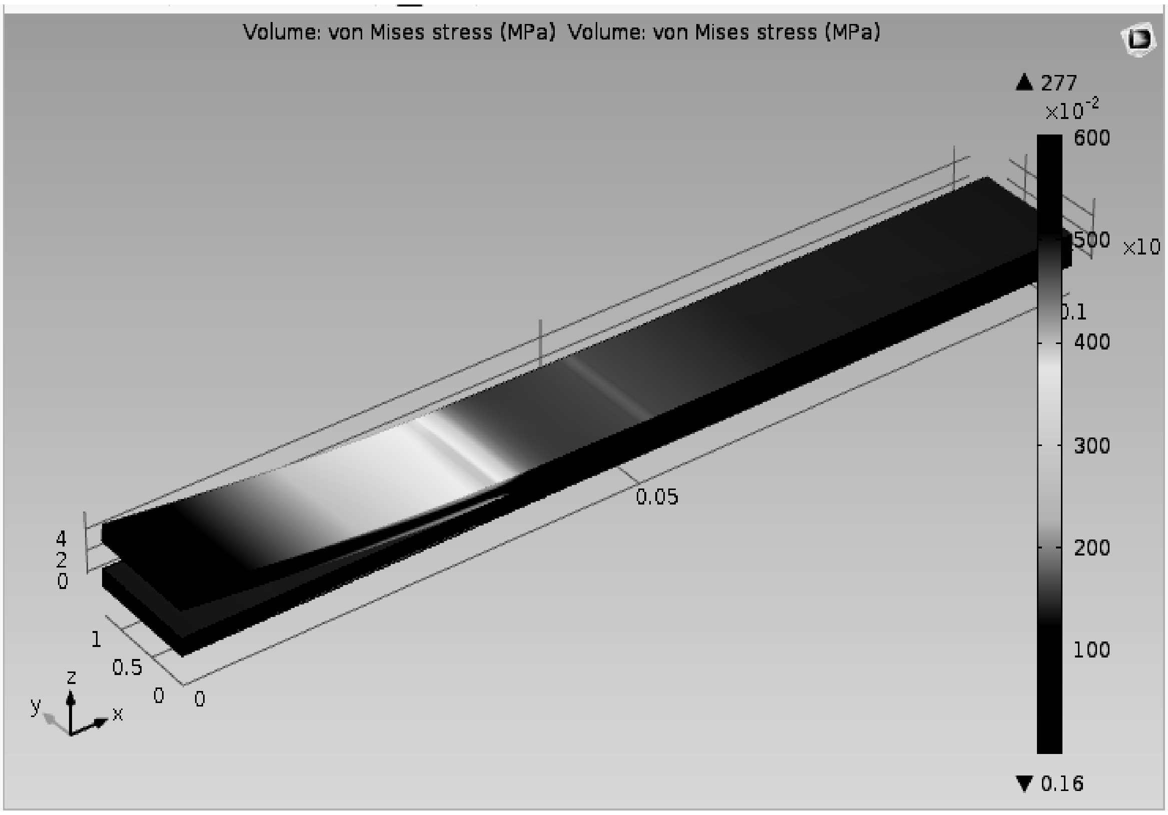

Fig. 11. The model stress chart for β=0,2 in COMSOL [Own elaboration]

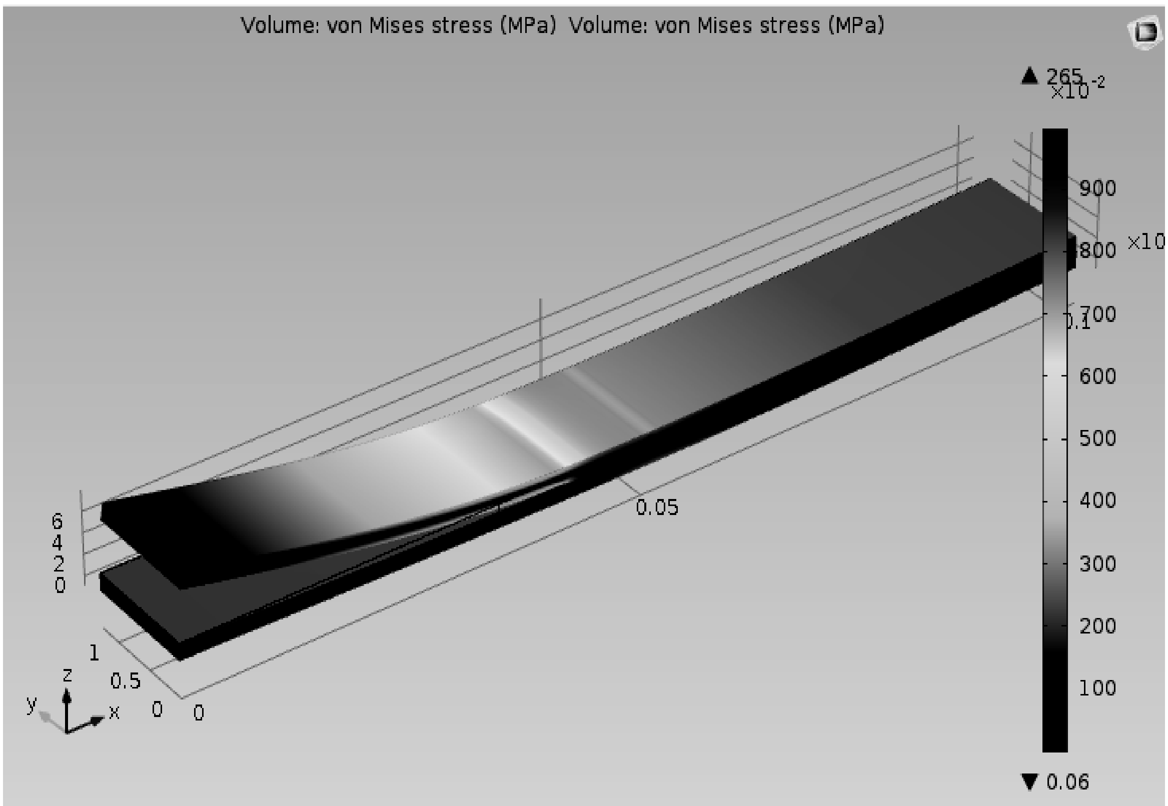

Fig. 12. The model stress chart for β=0,5 in COMSOL [Own elaboration]

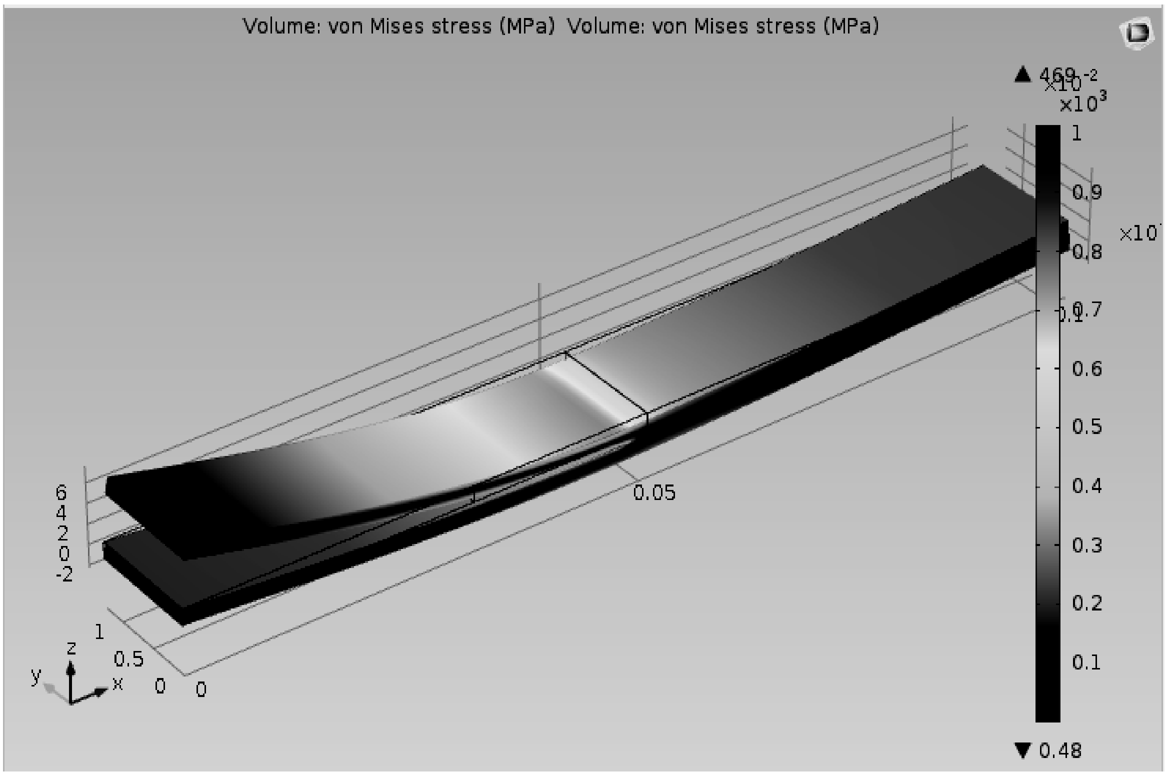

Fig. 13. The model stress chart for β=0,8 in COMSOL [Own elaboration]

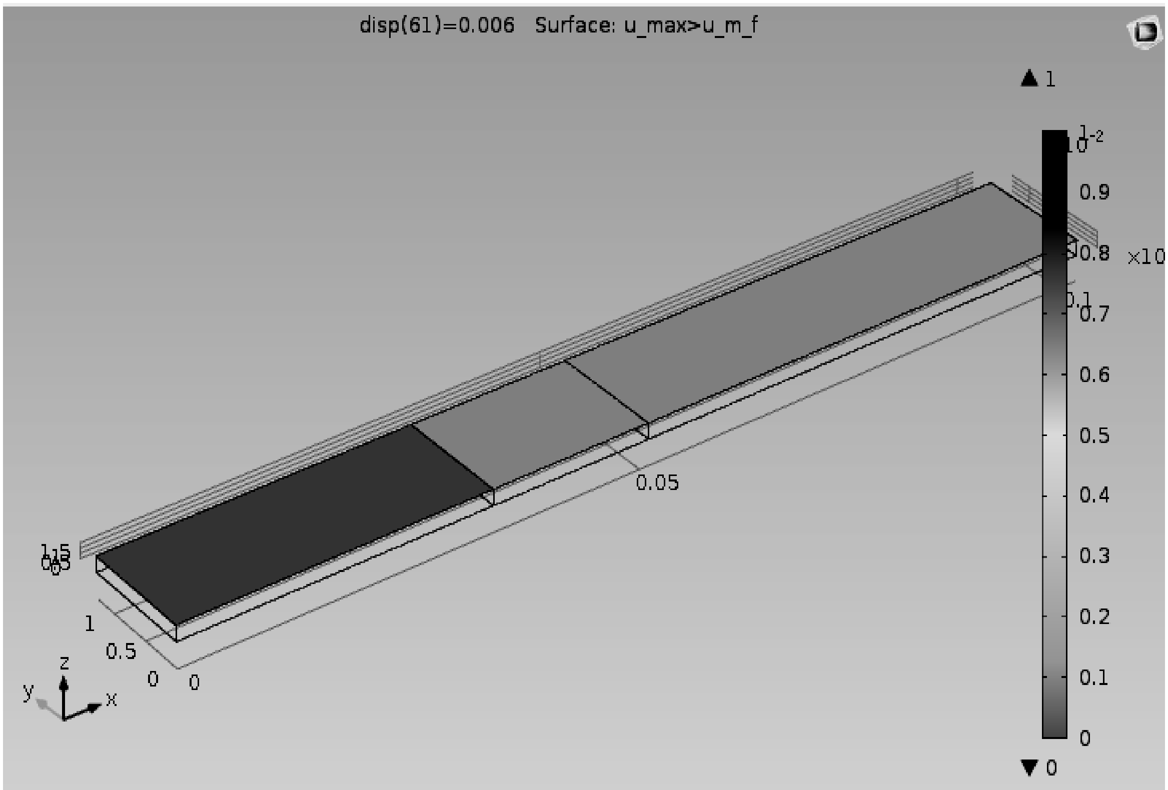

Fig. 14. The model deformation chart for β=0,2 in COMSOL [Own elaboration]

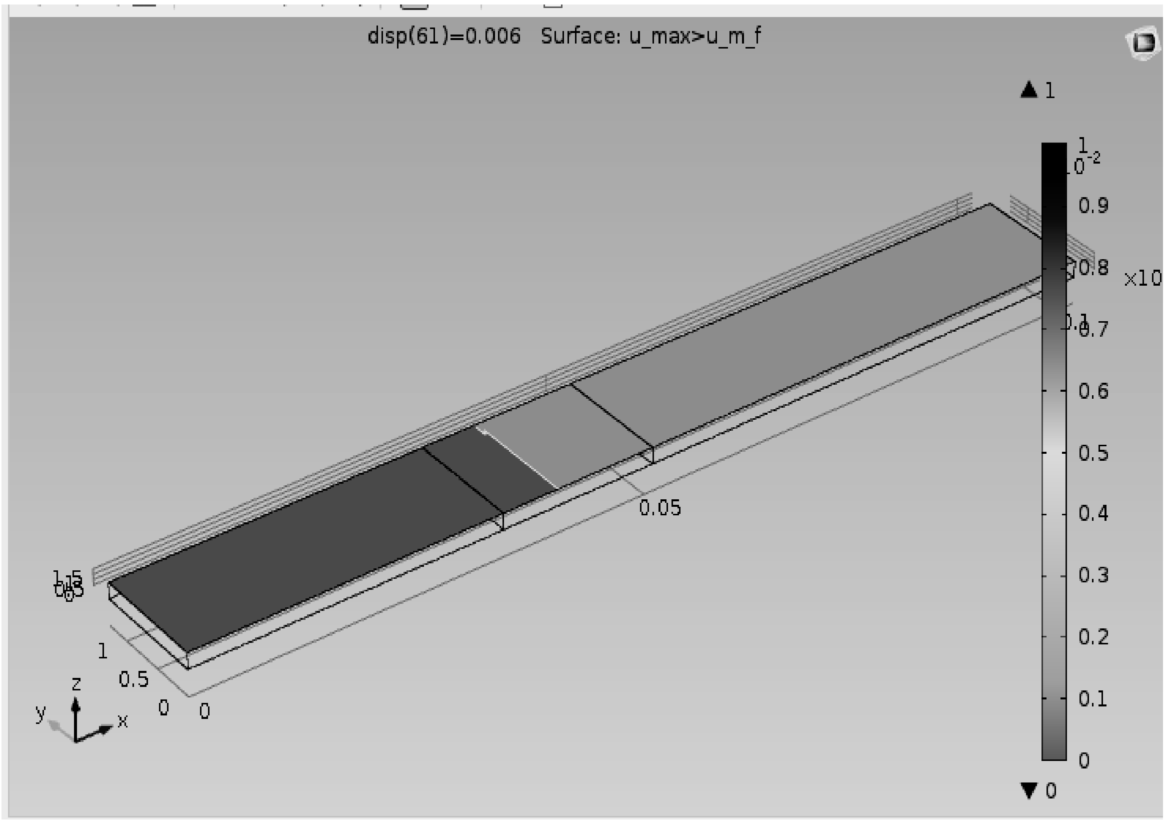

Fig. 15. The model deformation chart for β=0,5 in COMSOL [Own elaboration]

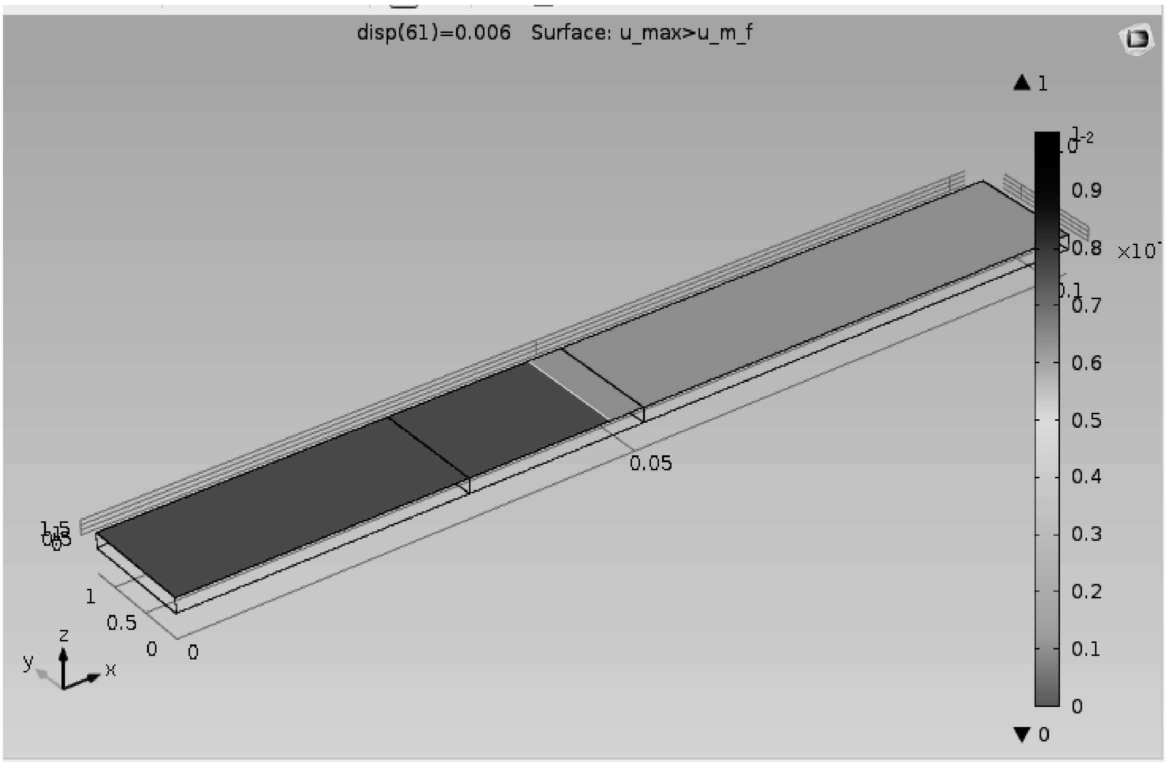

Fig. 16. The model deformation chart for β=0,8 in COMSOL [Own elaboration]

On the basis of the presented results it can be stated that the greater the distance between the force applied and the middle of the composite, the faster (upon lesser displacement of leverage downward) delamination takes place (as the force increases).

CONCLUSIONS

The modelling process presented in this work has allowed for the presentation of delamination of material AS4/PEEK depending on the value of the load force applied.

The delamination modelling has led to the following conclusions:

1. The experiments conducted have made it possible to conclude that it is possible to present the delamination of a layered composite using the Finite Element Method [9, 18, 25, 34];
2. As the distance between the force applied and the middle of the beam grows, the demand for delaminating force decreases, and displacement of the load point increases. This is due to the application of the leverage phenomenon in the model.
3. The size of the delaminated area depends on the size of the force, and thus on the distance between the force and the middle point of the laminate. As the force applied increases, the delamination area increases. Greater force leads to faster delamination from the fracture point up to the end of the laminate, and thus the process of increasing of delamination in the opposite direction is also initiated earlier.
4. On the basis of the results obtained with regard to the size of the force applied, it was concluded that the numerical model represented well the mathematical model presented by Comanho. The negative result errors were due to the increased sensitivity of the software to the laminate fracture phenomenon, occurring during the experiment. Thanks to good representation of the model, it can be used interchangeably with numerical calculations.

REFERENCES

1. **Airoldi A., Baldi A., Bettini P., Sala G. 2015.** Efficient modelling of forces and local strain evolution during delamination of composite laminates, Composites Part B 4/2015, Milano, pp. 137–149.
2. **Alfano, G., Crisfield, M. A. 2001.** Finite element interface models for the delamination analysis of laminated composites: mechanical and computational issues. International Journal for Numerical Methods in Engineering, 50(7), pp. 1701–1736.
3. **Balonek K., Gozdur S. 1999.** Wprowadzenie do Metody Elementu Skończonego [online], AGH, Uczelniane Wydawnictwo Naukowo – Dydaktyczne, Kraków – dostęp 14.03.2017. Dostępny w internecie: http://213.184.15.149/wwwkipr/markowski/techniki/1.%20 Wprowadzenie%20do%20MES.pdf.
4. **Bielski J. 2010.** Wprowadzenie do inżynierskich zastosowań MES, Wydawnictwo Politechniki Krakowskiej, Kraków, S. 10–11.
5. **Gupta A.G. 1973.** Layered composite with a broken laminate, International Journal of Solids and Structures 9(10), Pennsylvania, pp. 1845–1864.
6. **Budzyński A. 2006.** Krótki wstęp do zastosowania Metody Elementów Skończonych (MES)do numerycznych obliczeń inżynierskich [online], biuletyn GM ViewSYSTEM 5/2006, Wrocław – dostęp 14.03.2017. Dostępny w internecie: http://www.knse.pl/publikacje/65.pdf.
7. **Camanho P. P., Davila C. G., De Moura M. F. 2003.** Numerical Simulation of Mixed-mode Progressive Delamination in Composite Materials, Journal of composite materials 37.16, New York, pp. 1415–1438.
8. **Chróścielewski J., Makowski J., Pietraszkiewicz W. 2004.** Statyka i dynamika powłok wielopłatowych. Nieliniowa teoria i metoda elementów skończonych, Instytut Podstawowych Problemów Techniki Polskiej Akademii Nauk, Warszawa, S. 343.
9. **Corigliano A. 1993.** Formulation, identification and use of interface models in the numerical analysis of composite delamination. International Journal of Solids and Structures, 30(20), pp. 2779–2811.
10. **Daudeville L., Allix O., Ladeveze P. 1995.** Delamination Analysis by Damage Mechanics: Some Applications, Composite Engineering 9, Francja, pp. 17–24.
11. **Davim, J. P., Rubio, J. C., Abrao, A. M. 2007.** A novel approach based on digital image analysis to evaluate the delamination factor after drilling composite laminates. Composites Science and Technology, 67(9), pp. 1939–1945.
12. Departament of Defense, Composites Materials Handbook [online], United States of America 1999, 105 – dostęp 14.03.2017. Dostępny w internecie: http://snebulos.mit.edu/ projects/ reference/MIL-STD/MIL-HDBK-17-2F.pdf.
13. **Grilo T. J., Paulo R. M. F., Silva C. R. M., Davim J. P. 2013.** Experimental delamination analyses of CFRPs using different drill geometries. Composites Part B: Engineering, 45(1), pp. 1344–1350.
14. **Jacques, S., De Baere, I., Van Paepegem, W. 2015** Analysis of the numerical and geometrical parameters influencing the simulation of mode I and mode II delamination growth in unidirectional and textile composites. Applied Composite Materials, 22(6), pp. 637–668.
15. **Kargarnovin M. H., AhmadianM. T., Jafari-Talookolaei R. A., Abedi M. 2013.** Semi-analytical solution for the free vibration analysis of generally laminated composite Timoshenko beams with single delamination. Composites Part B: Engineering, 45(1), pp. 587–600.
16. **Katunin A., Wronkowicz A. 2015.** Directionality detection of delaminations basing on analysis of CT slices using wavelet and Hough transforms-based algorithm [online]. Diagnostyka, Vol. 16, No. 2 – dostęp 14.03.2017. Dostępny w internecie: file://C:/Users/Karol/Downloads/ katunin_wronkowicz_directionality_2_2015.pdf.
17. **Krupa K. 2009.** Modelowanie, symulacja i prognozowanie, Wydawnictwo WNT, Warszawa, 20–22.
18. **Lodwik D., Malesa W. 2014.** An Analysis of Selected Container Structures with Built-In Multi-Layer Composite Sheets with the Use of FEM. *TEKA.* COMMISSION OF MOTORIZATION AND ENERGETICS IN AGRICULTURE, Vol. 14, No. 3, pp. 73–76.
19. **Łaczek S. 2011.** Modelowanie i analiza konstrukcji w systemie MES ANSYS v. 1, Wydawnictwo Politechniki Krakowskiej, Kraków, S. 30–31.
20. **Mazurkiewicz Ł., Małachowski J., Damaziak K. 2011.** Porównanie metod modelowania delaminacji w kompozytach warstwowych, X Forum Inżynierskie ProCAx, Sosnowiec, pp. 1–7 – dostęp 14.03.2017. Dostępny w internecie: http://www.procax.org.pl/pliki/Art_17_2011_ Mazurkiewicz_Malachowski_Damaziak.pdf.

21. **Mieszkalski L. 2015**. Methodological aspects of development of a 3D model of a broad bean seed huller. Part I. The broad bean seed hulling concept.Ann. Warsaw Univ. of Life Sci. – SGGW, Agricult. 66, S. 61–69.
22. **Milenin A. 2010.** Podstawy Metody Elementów Skończonych. Zagadnienia termomechaniczne, AGH, Uczelniane Wydawnictwo Naukowo – Dydaktyczne, Kraków, S. 10–11.
23. **Nasiri M., Soltani M., Motlagh A. M. 2013.** Determination of agricultural soil compaction affected by tractor passing using 3D finite element, Agricultural Engineering International: CIGR Journal, Tehran, pp. 11–16.
24. **Niezgodziński T., Niezgodziński M.E. 2010.** Wytrzymałość materiałów, Wydawnictwo Naukowe PWN, Warszawa, p. 35.
25. **Nguyen V. P., Nguyen-Xuan H. 2013.** High-order B-splines based finite elements for delamination analysis of laminated composites. Composite Structures, 102, pp. 261–275.
26. **Ponikiewski T., Katzer J. 2014.** Mechanical Characteristics of Green SCC Modified by Steel and Polymer Fibres.Annual Set The Environment Protection Rocznik Ochrona Środowiska,vol. 16, S. 173–185.
27. **Shi Y., Pinna C., Soutis C. 2014.** Modelling impact damage in composite laminates: A simulation of intra- and inter-laminar cracking, Composite Structures 7, Sheffield 2014, pp. 10–19.
28. **Skrobol A. 2010.** Programy do analizy metodą elementów skończonych, Projektowanie konstrukcyjne inżynierskie 1/2 (28/29) 2010, Warszawa, S. 3–6.
29. **Szeląg D., Bajurko P., Czarnocki P. 2012.** Modelowanie numeryczne rozwoju delaminacji w warunkach obciążeń cyklicznych, Prace Instytutu Lotnictwa, Warszawa, S. 189–193.
30. **Tabatabaian M**. **2014.** COMSOL for Engineers, Wydawnictwo Mercury Learning & Information, Unitet States, p. 11.
31. **Tay T. E. 2003.** Characterization and analysis of delamination fracture in composites: an overview of developments from 1990 to 2001. Applied Mechanics Reviews, 56(1), pp. 1–32.
32. **Wilk J. 2015.** Assessing the hazard of delamination propagation in composites using numerical analysis. Composites Theory and Practice, p. 15.
33. COMSOL Multiphysics Dostępny w internecie: www.comsol.com.
34. **Zou Y., Tong L. P. S. G., Steven G. P. 2000.** Vibration-based model-dependent damage (delamination) identification and health monitoring for composite structures – a review. Journal of Sound and Vibration, 230(2), pp. 357–378.